# Pannexin 1 and pannexin 3 are glycoproteins that exhibit many distinct characteristics from the connexin family of gap junction proteins

**Silvia Penuela[1], Ruchi Bhalla[1], Xiang-Qun Gong[2], Kyle N. Cowan[3], Steven J. Celetti[2], Bryce J. Cowan[4], Donglin Bai[2], Qing Shao[1] and Dale W. Laird[1,*]**

[1]Departments of Anatomy and Cell Biology, [2]Physiology and Pharmacology and [3]Surgery, University of Western Ontario, London, ON, N6A 5C1, Canada
[4]Department of Dermatology and Skin Science, University of British Columbia, Vancouver, BC, Canada
*Author for correspondence (e-mail: Dale.laird@schulich.uwo.ca)

*Accepted 9 August 2007*
*Journal of Cell Science 120, 3772-3783 Published by The Company of Biologists 2007*
*doi:10.1242/jcs.009514*

## Summary

**Pannexins are mammalian orthologs of the invertebrate gap junction proteins innexins and thus have been proposed to play a role in gap junctional intercellular communication. Localization of exogenously expressed pannexin 1 (Panx1) and pannexin 3 (Panx3), together with pharmacological studies, revealed a cell surface distribution profile and life cycle dynamics that were distinct from connexin 43 (Cx43, encoded by *Gja1*). Furthermore, N-glycosidase treatment showed that both Panx1 (~41-48 kD species) and Panx3 (~43 kD) were glycosylated, whereas N-linked glycosylation-defective mutants exhibited a decreased ability to be transported to the cell surface. Tissue surveys revealed the expression of Panx1 in several murine tissues – including in cartilage, skin, spleen and brain – whereas Panx3 expression was prevalent in skin and cartilage with a second higher-molecular-weight species present in a broad range of tissues. Tissue-specific localization patterns of Panx1 and Panx3 ranging from distinct cell surface clusters to intracellular profiles were revealed by immunostaining of skin and spleen sections. Finally, functional assays in cultured cells transiently expressing Panx1 and Panx3 were incapable of forming intercellular channels, but assembled into functional cell surface channels. Collectively, these studies show that Panx1 and Panx3 have many characteristics that are distinct from Cx43 and that these proteins probably play an important biological role as single membrane channels.**

Key words: Communication, Connnexin, Gap junctions, Pannexin

## Introduction

The connexin gene family is comprised of 20 members in rodents (Willecke et al., 2002) and up until recently was considered to be the only family that encodes proteins responsible for gap junctional intercellular communication (GJIC). However, a second family of three genes encoding pannexins (*Panx1*, *Panx2* and *Panx3*) was discovered in vertebrates, and these proteins were found to have homology to the invertebrate gap junction proteins innexins (Panchin et al., 2000; Phelan, 2005). Given this relationship to innexins, pannexins were quickly proposed to be a second family of mammalian gap junction proteins (Panchin et al., 2000). *Panx1* has been reported in several rodent tissues at the mRNA level with a ubiquitous distribution similar to the most well-studied connexin, connexin 43 (Cx43, encoded by *Gja1*) (Barbe et al., 2006). Panx2, in contrast, appears to be more restricted to the central nervous system, whereas Panx3 has only been found in expressed sequence tags from libraries of osteoblasts, synovial fibroblasts, cartilage and skin (Baranova et al., 2004).

It is now well understood that connexin-based gap junction channels are permeable to the diffusion of ions and small molecules between adjacent cells (Alexander and Goldberg, 2003). Six connexins form a hemichannel (or connexon) and two apposed hemichannels form a functional intercellular channel (Bruzzone et al., 1996; Laird, 1996). Although connexins and pannexins show no sequence homology, like connexins, pannexins are predicted to be polytopic, spanning the lipid bilayer four times to yield two extracellular loops and a cytoplasmic loop with the amino and carboxy terminals exposed to the cytoplasm. Similar to connexins, pannexins have conserved cysteine residues in putative extracellular loops; these loops might be involved in intramolecular disulfide bonding, as previously demonstrated for Cx43 (John and Revel, 1991). Cx43, the most prevalent connexin in vertebrate tissues (Goodenough et al., 1996), has been well characterized in its role as a gap junction protein, including a newly emerging role as a hemichannel conduit proposed to be important in ATP release (Evans et al., 2006; Goodenough and Paul, 2003). Cx43 is a phosphoprotein that exhibits a rapid turnover with a short half-life of only 1-3 hours (Beardslee et al., 1998; Laird et al., 1991). The rapid turnover of Cx43 gap junctions has also been well documented in vivo and by assessing the clearing of cell surface gap junctions upon a brefeldin A (BFA)-induced blockage of protein secretion (Laird et al., 1995).

The first evidence to support the functional role of pannexins as gap junction proteins was obtained in *Xenopus* oocytes, in which microinjected RNA encoding Panx1 revealed the formation of intercellular channels (Bruzzone et al., 2003). Just recently, a second report supported a gap junction role for

Panx1, because limited sulforhodamine dye transfer was observed in GJIC-deficient C6 glioma cells engineered to overexpress Panx1-GFP (Lai et al., 2007). Functional Panx1 intercellular channels were also implicated in the formation of $Ca^{2+}$-permeable gap junction channels (Vanden Abeele et al., 2006). Furthermore, a fourth report, which aimed to assess the functional importance of Panx1 in mammalian cells, revealed no dye transfer or electrical coupling in Panx1-expressing HeLa cells or mouse neuroblastoma (N2A) cells, respectively (Huang et al., 2007). One limitation of the early reports demonstrating a functional role of Panx1 in generating intercellular channels has been a systematic evaluation of the possibility that Panx1 expression might have induced a secondary response resulting in the elevation of endogenous connexins. This issue is particularly important because considerable evidence supports a role for Panx1 in forming functional single-membrane channels commonly referred to as hemichannels (half an intercellular channel) (Barbe et al., 2006; Bruzzone et al., 2005). Panx1 hemichannels were found to be mechanosensitive ATP and interleukin 1β-releasing channels (Bao et al., 2004; Pelegrin and Surprenant, 2006). Interestingly, Panx1 has also been found to form hemichannels in connexin-deficient erythrocytes (Locovei et al., 2006), in which classical gap junctions have never been reported. In addition, Panx1 hemichannel opening during stroke has been proposed to be involved in ischemic neuronal cell death (Thompson et al., 2006). Collectively, the evidence for Panx1 forming single-membrane channels is rather convincing, whereas the role of any pannexins in forming classical intercellular gap junctions remains an area of considerable debate. Furthermore, our understanding of Panx3 has lagged considerably, owing in large part to the lack of appropriate reagents to examine its biochemical and functional characteristics.

The finding that Panx1 and Panx3 can be co-expressed in the same mouse tissue, together with the fact that they have more homology with each other than to Panx2, prompted us to focus our studies on these two pannexins. The objective of the present study was to determine whether Panx1 and Panx3 exhibit the characteristics of classical connexin-based gap junctions.

## Results

### Sequence analysis and cloning of mouse Panx1 and Panx3

A ClustalW sequence alignment of mouse Panx1 and Panx3 revealed 59% conservation at the amino acid level with 154 identical residues. Four transmembrane (TM) domains were predicted by Toppred algorithms on both sequences. The domains with the highest sequence conservation were within the first third of the molecules (Fig. 1A). Two conserved cysteine residues are present in each of the predicted extracellular loops for both pannexins (Fig. 1A, asterisks). Net NGlyc1.0 (Blom et al., 2004) and NetPhos 2.0 (Blom et al., 1999) servers were used for the prediction of putative N-linked glycosylation sites as well as potential phosphorylation sites encoded within the sequence of both pannexins (Fig. 1B). The four potential glycosylation sites that are predicted for each pannexin (Table 1) do not take into consideration the predicted topology of the pannexins. If we assume that the transmembrane topology of pannexins is similar to that of connexins, the only meaningful glycosylation sites would be at asparagine 254 within the second extracellular loop of Panx1 and asparagine 71 encoded within the first extracellular loop of Panx3. Likewise if we only consider phosphorylation sites that are predicted to be within domains exposed to the cytoplasm, this would include six serine, one threonine and three tyrosine residues for Panx1; and seven serine, two threonine and one tyrosine residue for Panx3 (Table 2). Thus, Panx1 and Panx3 appear to be good candidates for being kinase substrates.

We cloned Panx1 and Panx3 with RT-PCR using mouse brain and osteoblast RNA (Fig. 1C). The major bands of approximately 1.4-1.5 kb were amplified and cloned into expression vectors, validated by sequencing and found to be identical to the annotated reference sequences. The smaller minor bands (Fig. 1C) were also cloned and their sequences were found to represent truncated versions of the complete transcripts.

### Subcellular localization and species of Panx1 and Panx3

Site-directed rabbit polyclonal antibodies were generated to two peptides derived from the C-terminus of mouse Panx1 (amino acid residues 395-409) and human PANX1 (residues 412-426) plus one peptide from mouse Panx3 (residues 379-392). When untagged Panx1 or Panx3 were transiently expressed in pannexin-deficient normal rat kidney (NRK) cells, immunolabeling revealed that both pannexins primarily distributed at the cell surface, including at cell boundaries in which the neighboring cell did not express pannexins (Fig. 2A). Likewise, at locations in which both contacting cells expressed pannexins, the fluorescence intensity increased with limited evidence of pannexin clustering into gap junction-like plaques. When GFP-tagged Panx1 was expressed in NRK cells, a similar localization profile was observed, suggesting that GFP did not significantly alter the distribution of Panx1 (Fig. 2B). However, when Panx3-GFP was expressed in NRK cells, the cell surface localization of Panx3 was replaced by an intracellular distribution. Panx3-GFP was typically found in a reticular pattern and co-localized with protein disulfide isomerase (PDI), a resident of the endoplasmic reticulum, indicating that the GFP tag interferes with normal Panx3 trafficking (Fig. 2B). To ascertain that the anti-Panx1 and -Panx3 antibodies were specific for their respective pannexins, antibody labeling was effectively eliminated when the anti-pannexin antibodies were mixed with their cognate peptides (Fig. 3A,C).

To determine the molecular species found in NRK cells upon the expression of Panx1 and Panx3, both Triton- and SDS-extraction-based cell lysates were prepared. Anti-Panx1 antibodies derived from the human (data not shown) and mouse sequences recognized multiple bands in the range of 41-48 kD in Panx1-expressing NRKs (Fig. 3B). All of these bands were eliminated by pretreatment of the antibodies with cognate peptides, suggesting that they represented different species of Panx1. Surprisingly, the anti-Panx3 antibody recognized a single broad band of ~43 kD (sometimes resolved as a doublet) in lysates from Panx3-expressing NRK cells that was eliminated by pre-adsorption with the cognate peptide (Fig. 3D). In the case of both Panx1 and Panx3, the addition of the GFP tag increased the size of the pannexins by approximately 27 kD (Fig. 3B,D).

### Panx1 and Panx3 exhibit cellular dynamics that are distinct from Cx43

Cx43 has a short half-life of only 1-3 hours (Beardslee et al., 1998; Laird, 1996; Laird et al., 1991) and, consistently, we have previously shown that Cx43 and Cx43-GFP gap junctions in rat breast tumor cells (BICR-M1R$_k$) are internalized from the cell surface within 6 hours when protein secretion is reversibly blocked with BFA (Laird et al., 1995; Thomas et al., 2005). Because BFA blocks all vesicular protein secretion (Lippincott-Schwartz et al., 1989) and pannexins are anticipated to be polytopic integral membrane proteins, BFA would be expected to also block pannexin secretion. To assess the rate of internalization of Panx1 and Panx3 with respect to Cx43, we co-expressed Panx1 and Cx43-GFP or Panx3 and Cx43-GFP in BICR-M1R$_k$ cells and evaluated the fate of both pannexins and Cx43-GFP after a 6-hour BFA treatment. Interestingly, no detectable decrease in cell surface Panx1 or Panx3 was observed. However, essentially all Cx43 gap junctions were lost from the cell surface with a concomitant increase in intracellular Cx43-GFP indicative of newly synthesized Cx43-GFP. Similar results were found for GFP-tagged Panx1 (data not shown). In untreated cells, Cx43-GFP was localized as punctate gap junction plaques at the cell surface, a distinct distribution pattern than that exhibited by either Panx1 or Panx3 when expressed in the same cell (Fig. 4). Collectively these studies

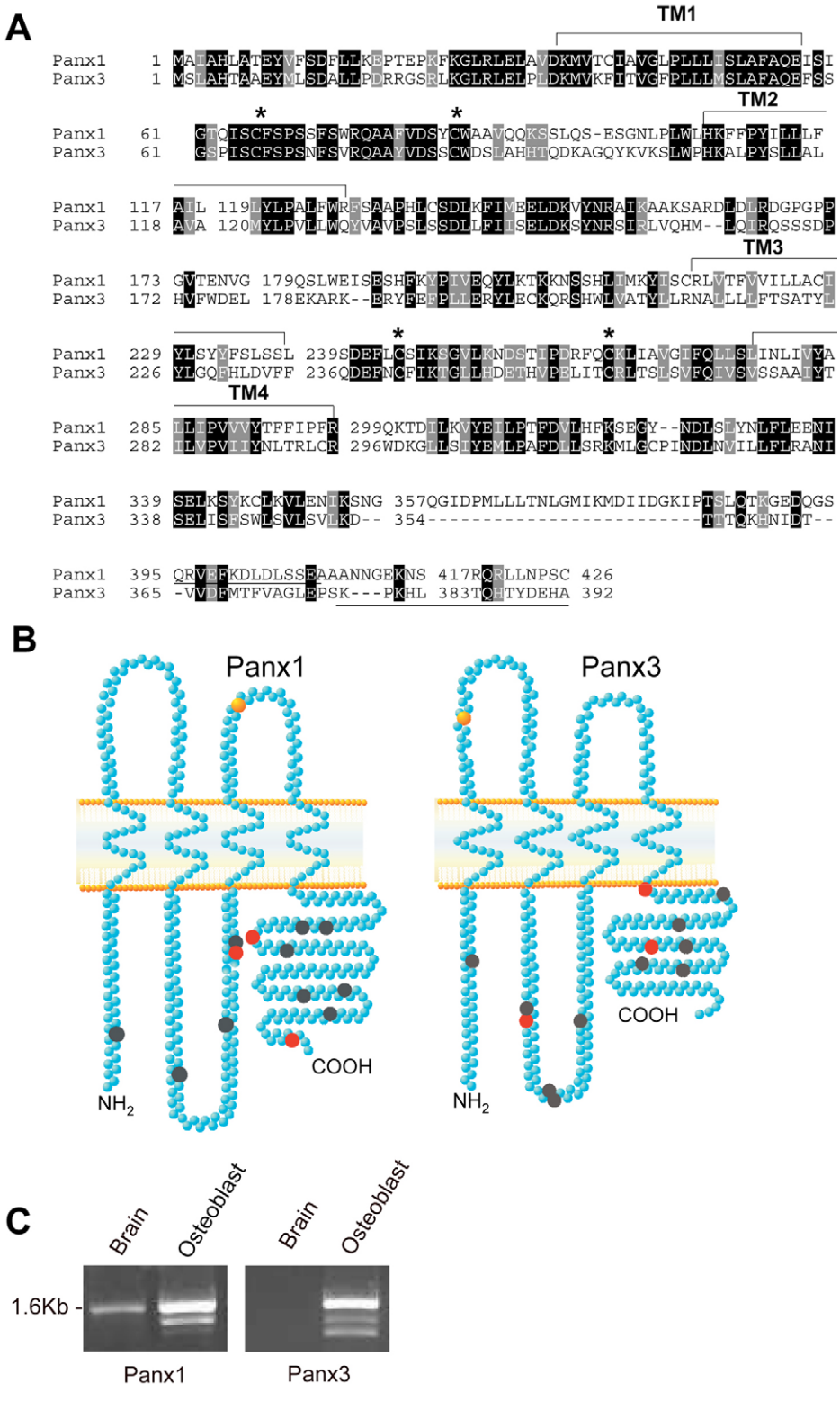


**Fig. 1.** Sequence analysis and cloning of mouse Panx1 and Panx3. (A) Sequence alignment of mouse Panx1 and Panx3. ClustalW alignment and BLAST analysis of the two protein sequences showed 41% identity at the amino acid level (black boxes). Some regions of high homology coincide with the four transmembrane domains (TM1-TM4) predicted by the Toppred algorithm. Asterisks mark conserved cysteine residues present in both predicted extracellular loops. Underlined sequences in the carboxyl-tail indicate the peptides used for the generation of polyclonal antibodies for each pannexin. Gray boxes indicate conserved amino acid substitutions. (B) Based on sequence analysis, both Panx1 and Panx3 are predicted to be polytopic and contain several predicted N-glycosylation (red and orange residues) and phosphorylation (black) sites. Orange residues indicate extracellular N-glycosylation sites used for site-directed mutagenesis. (C) RT-PCR products generated with specific primers designed to amplify the entire coding regions of each pannexin. A 1.5 kb band corresponding to Panx1 was amplified from both brain and osteoblast RNA from 3-week-old mice. A 1.4 kb Panx3 product was amplified from osteoblast RNA. All bands were sequenced to verify their identity as pannexin transcripts, but only the clones containing the entire coding region were engineered into expression vectors for further analysis.

**Table 1. Predicted N-glycosylation consensus sites**

| Pannexin | Position | Domain | Potential* |
|---|---|---|---|
| Panx1 | 204, NSSH | Intracellular loop | 0.30 |
| Panx1 | 254, NDST | Second extracellular loop | 0.39 |
| Panx1 | 337, NISE | Carboxyl tail | 0.53 |
| Panx1 | 423, NPSC | Carboxyl tail | 0.56 |
| Panx3 | 71, NFSV | First extracellular loop | 0.7 |
| Panx3 | 152, NRSI | Intracellular loop | 0.64 |
| Panx3 | 290, NLTR | Carboxyl tail | 0.66 |
| Panx3 | 336, NISE | Carboxyl tail | 0.55 |

*Predicted glycosylation potential (NetNGlyc 1.0 server). Threshold=0.5.

suggest that Panx1 and Panx3 exhibit distinct cellular kinetics from Cx43.

To further compare the kinetic properties of pannexins and Cx43, Panx1 and Cx43 expression was examined in BICR-M1$R_k$ cells under conditions in which protein synthesis was inhibited by cycloheximide (CHX). In agreement with the BFA results and when compared to untreated cells, immunoblot analysis of Panx1 levels revealed no significant difference ($P$=0.4980) between the banding profile at 2, 4, 6 and 8 hours of CHX treatment (Fig. 5A), whereas there was an overall time-dependent decrease in Cx43 levels following CHX treatment (Fig. 5B).

## Panx1 and Panx3 are glycosylated when expressed in NRK cells

Based on the fact that *Panx1* and *Panx3* encode consensus sites for phosphorylation and glycosylation (Tables 1, 2), we speculated that multiple bands observed in Panx1-expressing cells and the broad band observed for Panx3 might be due to phosphorylation or N-linked glycosylation. It is widely known that the multiple band species observed in Cx43-expressing cells is due to differential states of phosphorylation (Solan and Lampe, 2005); thus, we first treated NRK cells and Panx1-expressing NRK cells with alkaline phosphatase to determine whether the multiple Panx1 species could be reduced to only one species. Although the SDS-PAGE banding pattern of Panx1 did not change upon alkaline phosphatase treatment, Cx43 was reduced to one species (Fig. 6A), indicating that multiple Panx1 protein bands are not due to phosphorylation. Likewise, alkaline phosphatase treatment did not change the SDS-PAGE band pattern for Panx3 (data not shown). However, when cell lysates from Panx1- or Panx3-expressing NRK cells were treated with N-glycosidase F, the slower migrating Panx1 species accumulated into the fastest migrating species, strongly suggesting that the multiple species observed in Panx1-expressing cells were due to N-linked glycosylation (Fig. 6B). Likewise, the one Panx3 species substantially migrated further upon N-glycosidase treatment, suggesting that all of Panx3 was glycosylated. As a positive control, the glycoprotein transferrin was shown to migrate faster when treated with N-glycosidase F. Our data indicate that at least two of the three pannexin members are highly glycosylated, a unique property that distinguishes them from connexins.

To determine the potential effect of glycosylation on the subcellular localization of pannexins, we generated expression constructs (*Panx1*$^{N254Q}$ and *Panx3*$^{N71Q}$) that eliminated the most likely site for N-linked glycosylation in each pannexin. The mutant proteins were transiently expressed in NRK cells in parallel with the parental pannexin proteins, and immunolabeling revealed that a subpopulation of both mutants reached the cell surface, although they localized more extensively to intracellular compartments (Fig. 7A). The corresponding cell lysates were treated with N-glycosidase F and immunoblots revealed that both mutants appeared not to be glycosylated (Fig. 7B,C).

## Heterogeneous distribution of Panx1 and Panx3

Affinity-purified anti-Panx1 and anti-Panx3 antibodies were used to examine the expression profile of these pannexins in several tissues obtained from 3-week-old C57/BL6 mice. Interestingly, the band profiles for Panx1 suggest that this

**Table 2. Predicted intracellular phosphorylation sites**

| Pannexin | Position | Context | Domain | Score* | Predicted residue |
|---|---|---|---|---|---|
| Panx1 | 159 | KAAKSARDL | Intracellular loop | 0.99 | S |
| Panx1 | 206 | KKNSSHLIM | Intracellular loop | 0.73 | S |
| Panx1 | 328 | YNDLSLYNL | Carboxyl tail | 0.58 | S |
| Panx1 | 343 | SELKSYKCL | Carboxyl tail | 0.99 | S |
| Panx1 | 394 | EDQGSQRVE | Carboxyl tail | 0.92 | S |
| Panx1 | 405 | DLDLSSEAA | Carboxyl tail | 0.98 | S |
| Panx1 | 387 | TSLQTKGED | Carboxyl tail | 0.78 | T |
| Panx1 | 10 | LATEYVFSD | N-terminus | 0.72 | Y |
| Panx1 | 192 | SHFKYPIVE | Intracellular loop | 0.66 | Y |
| Panx1 | 324 | KSEGYNDLS | Carboxyl tail | 0.94 | Y |
| Panx3 | 23 | DRRGSRLKG | N-terminus | 0.99 | S |
| Panx3 | 150 | ELDKSYNRS | Intracellular loop | 0.96 | S |
| Panx3 | 167 | QIRQSSSDP | Intracellular loop | 0.99 | S |
| Panx3 | 168 | IRQSSSDPH | Intracellular loop | 0.93 | S |
| Panx3 | 303 | KGLLSIYEM | Carboxyl tail | 0.96 | S |
| Panx3 | 315 | FDLLSRKML | Carboxyl tail | 0.57 | S |
| Panx3 | 342 | SELISFSWL | Carboxyl tail | 0.5 | S |
| Panx3 | 357 | KDTTTQKHN | Carboxyl tail | 0.66 | T |
| Panx3 | 364 | HNIDTVVDF | Carboxyl tail | 0.88 | T |
| Panx3 | 186 | RKERYFEFP | Intracellular loop | 0.95 | Y |

*Phosphorylation score (NetPhos 2.0 Server). Max.=1.0.

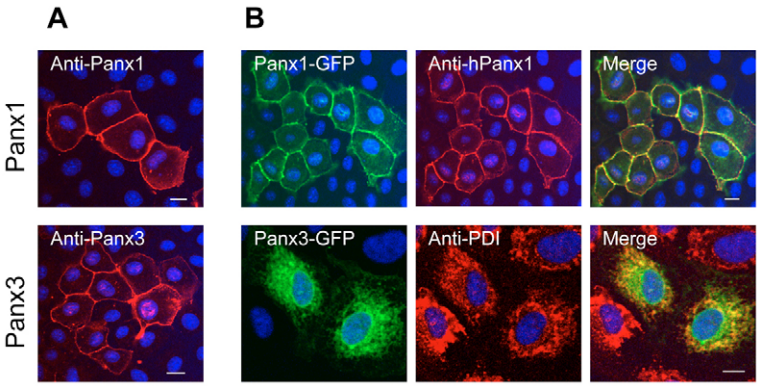


**Fig. 2.** Panx1 and Panx3 are localized to the cell surface when expressed in NRK cells. Confocal microscopic images of NRK cells expressing untagged Panx1 or Panx3 (A) or GFP-tagged Panx1 or Panx3 (B). Immunolabeling with mouse (anti-Panx1) and human (anti-hPANX1) antibodies revealed that Panx1 and Panx1-GFP were found at the cell surface with increased intensity at cell-cell interfaces when both cells expressed Panx1 or Panx1-GFP. Similar to that observed for Panx1, Panx3 displayed cell surface localization. However, Panx3-GFP was retained within the cell and colocalized with protein disulfide isomerase, an endoplasmic reticulum protein. Bars, 10 μm.

protein is heterogeneously glycosylated and found in brain, spleen, skin and cartilage (Fig. 8A). Low, but detectable, Panx1 signals were found in lung, kidney and heart ventricles (Fig. 8A), although this might be due in part to non-specific binding, as revealed by the light bands that remain when cognate peptides were used in competition assays (Fig. 8A). Because Panx1 has been reported to be present in erythrocytes (Locovei et al., 2006) and endothelial cells (Dvoriantchikova et al., 2006a; Dvoriantchikova et al., 2006b), it is possible that any low levels of Panx1 expression might be due to the presence of blood vessels and not due to the major cell type that constitutes the tissue. Because of the strong Panx1 signal in spleen, we speculated that this pannexin might also be prevalent in other lymphoid organs. Therefore, we probed the thymus of neonatal mice and found that all species of Panx1 were present (Fig. 8A). Panx3, in contrast, was found in cartilage and skin with low

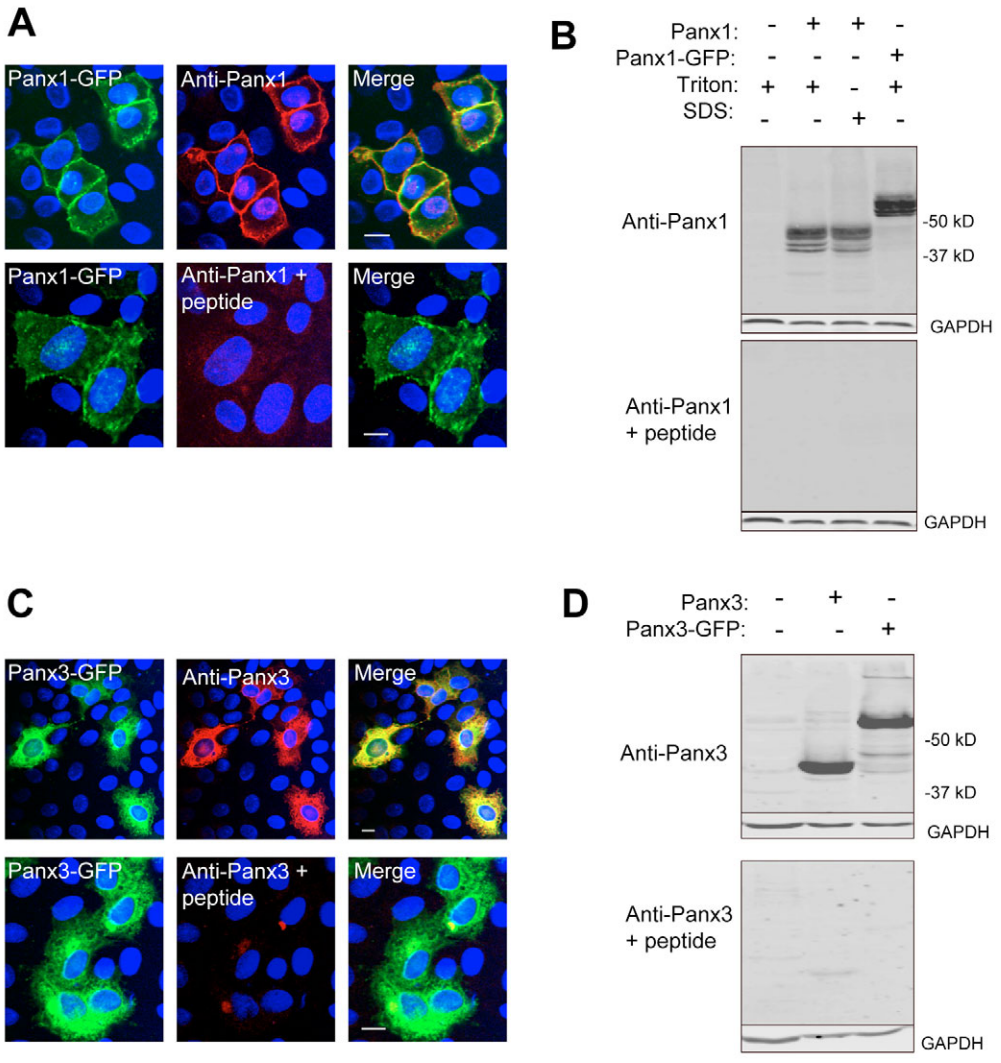


**Fig. 3.** Antibody specificity and Panx1 and Panx3 species. Affinity-purified anti-Panx1 antibody shows high specificity to Panx1 both in immunolabeling (A) and western blot (B) when pre-adsorbed with cognate peptides. (B) Multiple species of Panx1 at ~41-48 kD and Panx1-GFP at ~70-80 kD were detected. (C,D) Affinity-purified anti-Panx3 antibody revealed high specificity to Panx3 both in immunolabeling (C) and western blot (D) when pre-absorbed with cognate peptides. Only one species of Panx3 or Panx3-GFP was detected at ~43 kD or ~70 kD, respectively. Anti-GAPDH was used to assess gel loading. Bars, 10 μm.

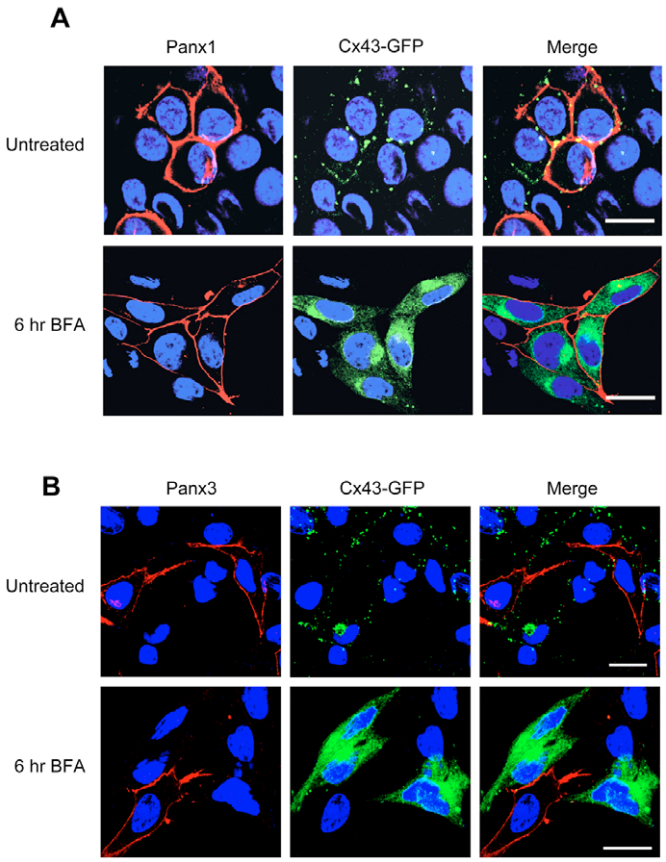


**Fig. 4.** Unlike Cx43-GFP, cell surface Panx1 and Panx3 localization is unaffected by BFA treatment. BICR-M1R$_k$ cells co-expressing Cx43-GFP and Panx1 (A) or Panx3 (B) were treated with 5 μg/ml BFA for 6 hours. After treatment, Cx43-GFP plaques internalized from the cell surface and newly biosynthesized Cx43-GFP accumulated within intracellular compartments, whereas the localization of Panx1 and Panx3 remained unchanged. The experiment shown is representative of three independent repeats. Bars, 20 μm.

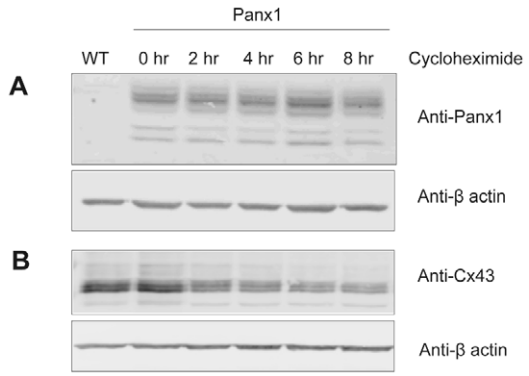


**Fig. 5.** Panx1 expression levels were unchanged during cycloheximide treatment. BICR-M1R$_k$ cells expressing endogenous Cx43 and exogenous Panx1 were exposed to 20 μg/ml of CHX for 2, 4, 6 and 8 hours and immunoblotted for Panx1 (A) and Cx43 (B). When compared to un-treated cells (0 hr), immunoblot analysis of Panx1 revealed no significant difference ($P$=0.4980) between the banding profile at 2, 4, 6 and 8 hours of CHX treatment. However, given the known short half-life of Cx43, the level of Cx43 consistently diminished following 2, 4, 6 and 8 hours of CHX treatment. β-actin was used as a protein loading control. The experiment shown is representative of three independent repeats. WT, wild type.

levels detected in the heart ventricle (Fig. 8B). Interestingly, in addition to monomeric Panx3 at ~43 kD, a second species was detected at ~70 kD that might represent a Panx3 dimer (Fig. 8B). It is notable that the ~70 kD band was also observed in organs in which the monomeric Panx3 was not detected: in lung, kidney, liver, thymus and spleen (Fig. 8C). Moreover, an additional band corresponding to a ~50 kD product was consistently present in kidney lysates probed with anti-Panx3 antibodies. Only a faint band for Panx3 was detected in the brain (Fig. 8C). All bands detected with the anti-Panx3 antibody were not observed in immunoblots when the antibody was pre-adsorbed with Panx3 cognate peptide (Fig. 8B,C).

### Differential expression and localization of endogenous pannexins in human skin and in the mouse spleen

Based on the results of the tissue survey, two tissues were chosen to further investigate the distribution of endogenous pannexins in vivo. First, human skin sections labeled with either human- or mouse-specific anti-Panx1 antibodies revealed Panx1 primarily in the stratum granulosum and spinosum, similar to Cx43 (Fig. 9A-C). By contrast, labeling with the antibody raised against Panx3 revealed a diffuse cellular distribution of Panx3 throughout the vital layers of the epidermis (Fig. 9E). Panx1 and Panx3 staining was confirmed to be specific because peptide competition experiments using both the human PANX1 antibody (Fig. 9D) and the mouse Panx3 antibody (Fig. 9F) as well as pre-immune serum controls (data not shown) revealed no specific labeling. Second, paraffin sections of murine spleen tissues immunolabeled with anti-Panx1 antibodies revealed a diffuse intracellular signal that was blocked by the cognate peptide (Fig. 9G,H). Collectively, these immunolocalization studies suggest that endogenous Panx1 and Panx3 exhibit at least two distinct localization profiles in mammalian tissues.

### Panx1 and Panx3 form functional plasma membrane channels in 293T cells

To assess the potential functional role(s) of Panx1 and Panx3, we first exposed wild-type human embryonic kidney (293T) cells or cells expressing Panx1 or Panx3 to extracellular sulforhodamine B to determine whether cell surface pannexin channels were formed that could uptake the fluorescent dye upon mechanical stimulation. Dramatic dye uptake was observed in 293T cells expressing Panx1 or Panx3 (Fig. 10A, left panels) but not in wild-type cells under physiological extracellular calcium concentrations. To ensure high transfection efficiency of Panx1 and Panx3, cells were co-transfected with plasmids encoding GFP, and only GFP-expressing cells were observed to uptake sulforhodamine. In parallel studies, the high expression of Panx1 and Panx3 was further revealed by immunolabeling (Fig. 10A, right panels). Finally, no uptake of the high-molecular-weight dye, dextran rhodamine (10,000 MW), was observed in pannexin-expressing or wild-type cells (Fig. 10A, inserts).

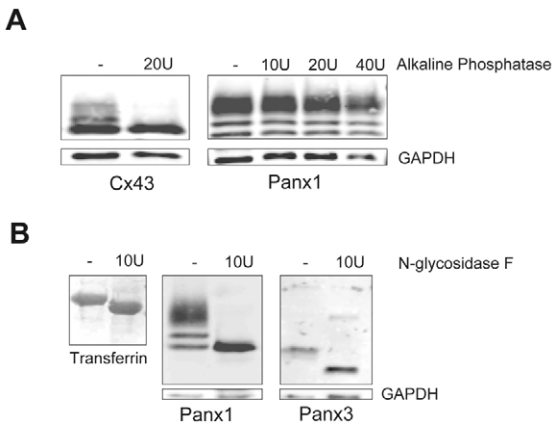


**Fig. 6.** Panx1 and Panx3 are highly glycosylated. (A) Whereas the multiple species of Cx43 were reduced to only one species upon alkaline phosphatase treatment, western blotting revealed that the multiple species of Panx1 remained unchanged by the same treatment. (B) Panx1 and Panx3 were found to be glycosylated, as revealed by protein-band shifts upon digestion with 10 units of N-glycosidase F. The glycoprotein transferrin was used as a positive control for N-glycosidase activity and anti-GAPDH antibody was used to assess gel loading.

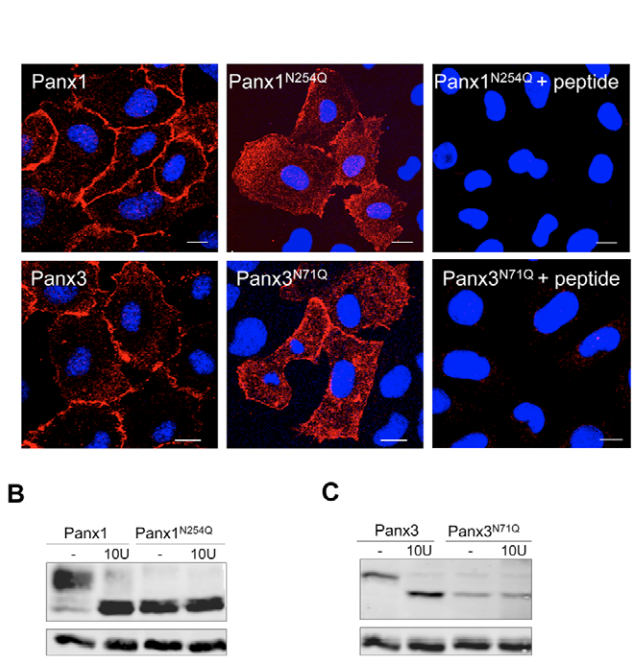


**Fig. 7.** Localization profile of N-glycosylation-defective mutants of Panx1 and Panx3. (A) A sub-population of N-glycosylation-defective pannexin mutants localized to the cell surface (red) but these proteins also exhibited an increase in intracellular localization when compared with their wild-type counterparts. Notice that specific anti-pannexin labeling was eliminated by pre-incubating the antibodies with cognate peptide. (B,C) Western blots revealed that the $Panx1^{N254Q}$ and $Panx3^{N71Q}$ mutants exist as species that are insensitive to 10 U of N-glycosidase treatment. Bars, 10 μm.

### Panx1 and Panx3 do not form intercellular channels in N2A cells

Because the functional status of Panx3 has not been well characterized, we first investigated whether this pannexin had the capacity to form intercellular channels in gap junction-deficient N2A cells. Wild-type N2A cells, N2A cells co-expressing Panx3 and the fluorescent protein DsRed (for visualization of transfected cells) or cells expressing Panx3 tagged with GFP were microinjected with Lucifer yellow. The transfer of Lucifer yellow to adjacent cells was assessed in over 85 microinjected cells repeated over three independent experiments. No significant difference was found between any of these three groups, suggesting that Panx3 does not assemble channels capable of intercellular Lucifer yellow dye transfer.

To more carefully examine the possibility that either Panx1 or Panx3 might form intercellular channels, we used double whole-cell patch-clamp recordings to assess the functional status of intercellular conductance of N2A cell pairs expressing Panx1, Panx3, Panx1-GFP or Panx3-GFP. Whereas both Cx43-GFP- and Cx26-GFP-expressing N2A cell pairs exhibited robust coupling, neither Panx1 nor Panx3 exhibited any significant increase in electrical coupling in comparison to that observed in non-transfected N2A cell pairs (Fig. 10B). These functional studies suggest that these two pannexins are incapable of forming homomeric intercellular channels at 48 hours post-transfection under our experimental conditions.

## Discussion

For over two decades the only known subunits of vertebrate gap junctions were members of the connexin family. However, with the discovery of pannexins, these novel proteins quickly became assigned as a putative second family of vertebrate gap junction proteins. However, this assignment was based on sequence homology to invertebrate gap junction proteins, innexins, and rested on the fact that Panx1 exhibited a low, but possibly meaningful, capacity to form intercellular channels in *Xenopus* oocytes (Bruzzone et al., 2003) and C6 glioma cells (Lai et al., 2007). In the event that pannexins are a second family of gap junction proteins, we postulated that they would exhibit many similar characteristics to connexins. Consequently, the focus of the present study was to assess the putative role of Panx1 and Panx3 as gap junction proteins in light of their expression characteristics, localization patterns, cellular kinetics, post-translational modifications and functional properties.

### Subcellular distribution of Panx1 and Panx3

One of the classical characteristics of connexin-based gap junctions has been their selective clustering of channels into dense arrays at locations of cell-cell contact (Goodenough et al., 1996). This phenomenon is usually accompanied by the lack of cell surface connexin staining in non-junctional membranes. Surprisingly, the distribution profile of exogenously expressed Panx1, Panx1-GFP and Panx3 revealed relatively even cell surface distribution profiles with limited clustering, whereas GFP-tagging Panx3 caused retention of this protein within the endoplasmic reticulum. Both Panx1 and Panx3 were easily identified at all cell surfaces regardless of whether the cell was in contact with another pannexin-expressing cell. In fact, the intensity of pannexin staining at locations of cell-cell contact provided no evidence for preferential recruitment or clustering of Panx1 or Panx3 at locations in which gap junctions were

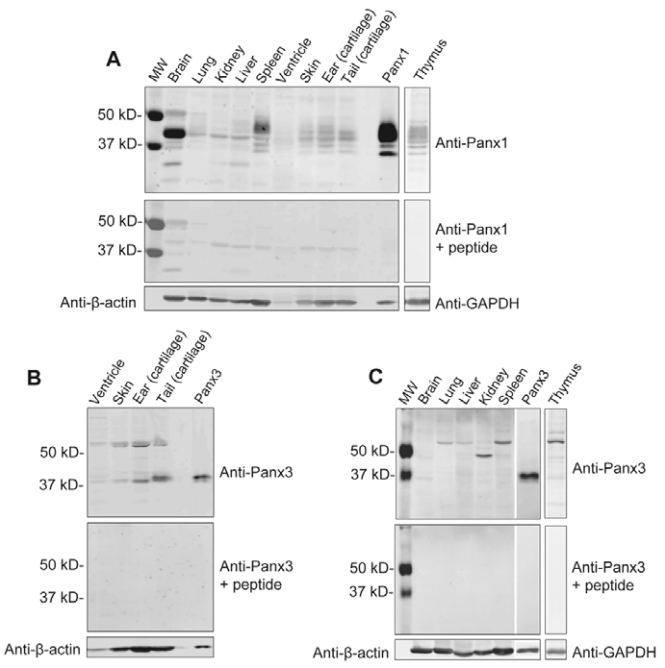


**Fig. 8.** Tissue expression of Panx1 and Panx3. Affinity-purified anti-Panx1 (A) and anti-Panx3 (B,C) antibodies were used to examine the expression of Panx1 and Panx3 in several tissue types from 3-week-old mice and in the thymus from neonatal mice. (A) Panx1 was prevalent in many murine organs and exhibited variable degrees of apparent glycosylation (~41-48 kD), whereas two putative isoforms of Panx3 (~43 kD and ~70 kD) were observed in skin, cartilage and heart ventricle (B). (C) Only a ~70 kD band was detected with the anti-Panx3 antibody in lung, liver, spleen and thymus, with a notable ~50 kD band present in kidney, whereas brain tissue exhibited little or no detectable Panx3. The tissues and Panx3 control used in C were obtained from the same gel. A peptide pre-adsorption assay eliminated most of the staining both for the Panx1 and Panx3 antibodies, indicating that these antibodies are specific for Panx1 and Panx3, respectively. Anti β-actin or anti-GAPDH was used as a loading control. MW, molecular weight standards; Ventricle, heart ventricle; Panx1, Panx1-expressing NRK cells; Panx3, Panx3-expressing NRK cells.

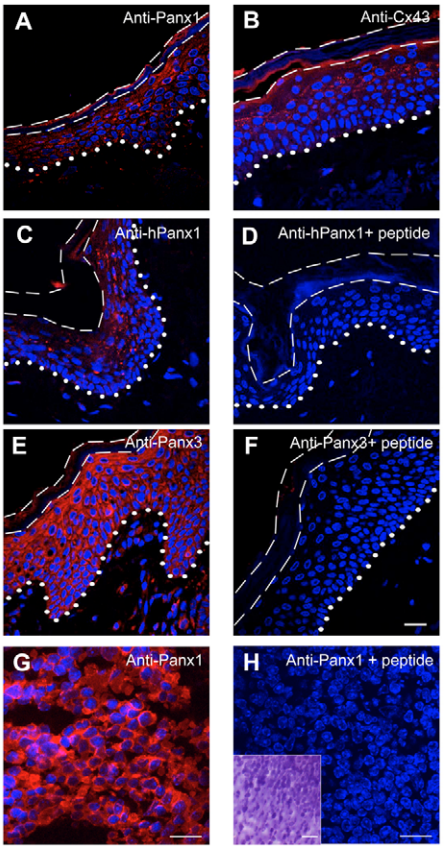


**Fig. 9.** Localization of endogenous Panx1 and Panx3 in normal human skin and mouse spleen. (A-F) Representative images of immunofluorescent labeling for Cx43, Panx1 and Panx3 (red) in normal human facial skin samples and counterstained with the Hoechst nuclear stain (blue). Labeling with either an antibody raised against mouse (A) or human (C) Panx1 identified Panx1 in a focal pattern distributed throughout the epidermis, but most abundantly in the layers of the stratum granulosum and spinosum. (D)Peptide competition with the human PANX1 antibody revealed the loss of specific labeling. (B) Cx43, localized for comparison, was present focally within the upper layers of the epidermis. (E,F) Immunolabeled Panx3 displayed a diffuse cellular distribution within the epidermis (E) that was eliminated by peptide competition (F). Broken lines denote the extent of the cornified layer; dotted lines indicate the edge of the epidermal vital layer. (G,H) Panx1 was localized in 3-week-old normal mouse spleen (G, red), whereas this staining pattern was eliminated after pre-adsorption with cognate peptide (H). Insert in H shows hematoxylin and eosin staining of a parallel spleen section. Bars, 20 μm.

expected to form. These findings are in keeping with the distribution profile of Panx1 in non-gap junction-forming erythrocytes and HeLa cells (Huang et al., 2007; Locovei et al., 2006). Furthermore, the broad cell surface distribution pattern of Panx1 would be consistent with Panx1 functionally acting as a single-membrane channel. However, evidence based on subcellular distribution characteristics of exogenously expressed pannexins alone is insufficient to conclude that pannexins do not form gap junctions in vivo. In fact, the distribution of endogenous pannexins in human skin and mouse spleen revealed that Panx1 exhibits two different profiles that appear to be tissue-specific and distinct from that observed in reference cell-culture models. Panx1 was found to exhibit a diffuse and uniform cellular pattern in mouse spleen, whereas it appeared more punctate throughout multiple layers of human epidermis. The latter punctate distribution pattern is in keeping with recent studies that reported punctate Panx1 aggregates in tissue sections of retina and mouse lenses (Dvoriantchikova et al., 2006a; Dvoriantchikova et al., 2006b), suggesting that the organization of Panx1 into junction-like complexes might occur in some tissues. Consequently, caution needs to be exercised in translating the Panx1 localization pattern observed in reference cell-culture models and native tissues. Given that our in vivo Panx1 labeling profiles were successfully eliminated by the competing peptides used to generate the antibodies, and two distinct antibodies to Panx1 were employed, we suggest that this represents true Panx1 localization. It is possible that other factors or molecules present in tissues but not in our reference cell models contribute to the organization and steady-state localization patterns observed. Similar to Panx1, Panx3 exhibited a more diffuse pattern in human skin sections than observed in reference cell models, in which it was typically

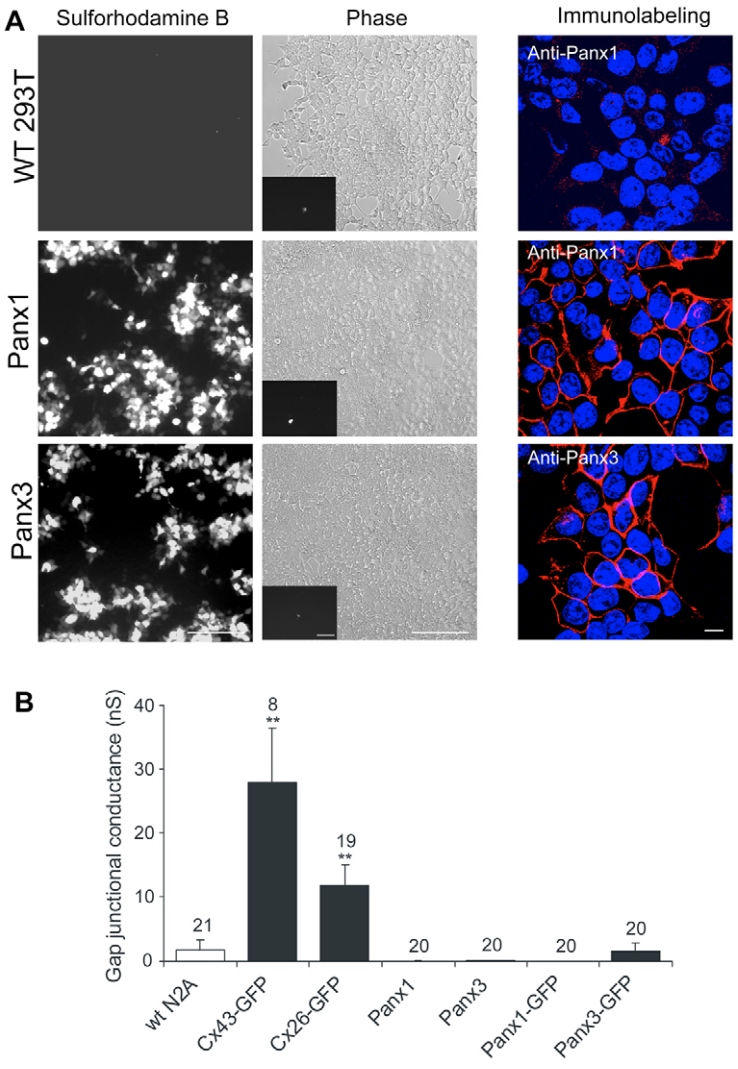


**Fig. 10.** Panx1 and Panx3 assemble into functional single-membrane channels in 293T cells but do not form functional intercellular channels in N2A cells. (A) Fluorescent micrographs of wild-type (WT) and pannexin-expressing 293T cells after sulforhodamine B dye uptake (left column: 20× objective). The middle column denotes the corresponding phase-contrast images, which includes the background uptake of the large control dye, dextran-rhodamine (inserts). (Right column) In parallel experiments, immunolabeling for pannexins (red) and counterstaining with Hoechst dye (blue) revealed the high pannexin transfection efficiency (63× oil objective). (B) GJIC-deficient N2A cells were engineered to transiently express Cx43-GFP, Cx26-GFP, Panx1-GFP or Panx3-GFP, or to co-express Panx1 or Panx3 and DsRed. Isolated N2A cell pairs with clear green or red fluorescence were chosen for dual whole-cell patch-clamp recordings 48 hours later to measure intercellular junctional conductance. The expression of Cx43-GFP and Cx26-GFP resulted in robust electrical coupling conductance between N2A cells, which was significantly higher than the coupling observed in paired control wild-type N2A (wt N2A) cells. However, both Panx1- and Panx3-expressing N2A cells exhibited no significant increase in electrical coupling above what was observed in wild-type N2A cells. Data were presented as mean±s.e.m.; $^{**}P<0.01$. The number presented over each column represents the *n* value for each experimental condition.

found evenly distributed at the cell surface. Again, these findings point to a complex mechanism of interactions that govern Panx1 and Panx3 distributions; one that will require more extensive investigation.

## Molecular Panx1 and Panx3 species

In the mouse genome, pannexin-encoding genes contain several introns and exons, allowing for potential alternative splicing events (Bruzzone et al., 2003), although splice variants of pannexins have yet to be demonstrated. *Panx1* and *Panx3* are located in mouse chromosome 9, and their orthologous genes map to chromosome 11 in the human genome with a conserved genomic spacing of 22-30 Mb, indicating potential synteny among species (Baranova et al., 2004). At the protein level, Panx1 and Panx3 are more homologous to each other than to Panx2 or to any of the invertebrate innexins (Baranova et al., 2004), and they encode many putative phosphorylation and glycosylation sites. Whereas Cx43 phosphorylation is highly regulated and responsible for the multiple species resolved on SDS-PAGE (Solan and Lampe, 2005), this is not the case for Panx1 or Panx3. Whether Panx1 or Panx3 are phosphoproteins remains unknown, but our results clearly reveal that both pannexins are N-linked glycosylated, a post-translational modification not found on any connexins. Because each pannexin has an N-linked glycosylation consensus site encoded within either the first or second extracellular loop, we predicted that these are the locations for such glycosylation events. Consequently, by substituting the N-linked glycosylation consensus site asparagines with glutamines, we were able to generate mutants that exhibited only the faster migrating species that were resistant to further de-glycosylation. The presence of complex carbohydrate chains on the extracellular-loop regions of Panx1 or Panx3 would be predicted to negatively affect the formation of intercellular channels by inhibiting the docking of hemichannels from apposing cell surface membranes. In the case of Panx1, this could be overcome if the one species of Panx1 that does not appear to be glycosylated can actually be transported to the cell surface and potentially be assembled into intercellular channels. Cell surface biotinylation of Panx1-expressing HeLa cells indicate that multiple species of Panx1 reach the cell surface (Huang et al., 2007) and, together with our findings that show that at least a sub-population of the unglycosylated Panx1$^{N254Q}$ mutant is capable of trafficking to the cell surface, these data raise the possibility that this species is the one that is capable of gap junctional intercellular communication. However, it is also possible that low levels of endogenous pannexins that are present in these cells could rescue the unglycosylated mutants and allow their trafficking to the cell surface. In the case of Panx3, the one species of Panx3 that was resolved by SDS-PAGE appears to be glycosylated and again a sub-population of the unglycosylated mutant can also reach the cell surface. However, these findings do not preclude the possibility that, in vivo, specific cell types with perhaps a different set of interacting proteins might in fact allow either glycosylated or unglycosylated pannexin species to aggregate into gap junction structures and participate in intercellular communication.

## Panx1 and Panx3 are less dynamic than Cx43

One of the unique characteristics of most connexin family

members is that their physiological regulation is not only at the level of gating the channels open or closed (Saez et al., 2005) but also at the level of gap junction formation and removal (Laird, 2006). The latter level of regulation is possible because most connexins have an unprecedented short half-life for polytopic plasma membrane proteins. In this regard, our studies in which protein synthesis or trafficking were blocked by pharmacological agents revealed that populations of both Panx1 and Panx3 remain on the cell surface for longer periods of time than Cx43 gap junctions, suggesting that they exhibit distinct dynamics from Cx43. Thus, Panx1 and Panx3 fail to meet a typical criterion expected of Cx43 gap junctions that are routinely regulated via processes leading to gap junction assembly, internalization and degradation.

### Heterogeneous tissue expression of Panx1 and Panx3

The tissue expression profile of Panx1 and Panx3 revealed several important findings. First, similar to Cx43 (Laird, 2006), Panx1 appears to be ubiquitously expressed in most mouse tissues at variable levels. Secondly, it is quite remarkable that the degree of Panx1 glycosylation is highly variable among the tissues. For instance, Panx1 is mostly glycosylated in the brain, even more highly glycosylated in the spleen and is weakly glycosylated in the skin and cartilage. This might suggest that the functional role of Panx1 in each of these tissues might be differentially regulated by the state of glycosylation. Thirdly, it is notable that spleen and neonatal thymus, which are enriched with gap junction-deficient lymphocytes and thymocytes, are rich in Panx1, suggestive of a potential non-gap junction role for Panx1 in these tissues. Similar to our initial reverse transcriptase (RT)-PCR results and to previous reports in the literature (Barbe et al., 2006), Panx1 appeared to be more abundant in mouse brain than Panx3, which was scarcely detectable. Finally, some tissues, such as skin and cartilage, expressed meaningful levels of both Panx1 and Panx3, suggesting that these pannexins might serve distinct roles in the same tissue. It remains to be determined whether the higher-molecular-weight species observed for Panx3 in different tissues correspond to an oligomer of the Panx3 or possibly to an isoform or splice variant of the gene that might play different tissue-specific roles.

### Panx1 and Panx3 assemble into functional cell surface channels in 293T cells but not into intercellular channels in N2A cells

In earlier studies, the overexpression of Panx1 in *Xenopus* oocytes was shown to form functional hemichannels and intercellular channels (Bruzzone et al., 2003). When co-injected with Panx2, but not Panx3, the functional properties of the Panx1 channels were attenuated, indicating a possible intermixing of Panx1 and Panx2. Importantly, inhibitors of connexin gap junction channels (e.g. carbexonolone, fluflenamic acid) also inhibit Panx1 intercellular channels (Bruzzone et al., 2005). Panx1 cell-cell-channel-forming properties as assessed by sulforhodamine transfer were also reported in GJIC-deficient C6 glioma cells that overexpressed Panx1-GFP (Lai et al., 2007), further supporting a gap junction channel role for Panx1. Panx1 was also implicated in the formation of $Ca^{2+}$-permeable gap junction channels in adjacent Panx1-expressing cells and in $Ca^{2+}$ leak through the endoplasmic reticulum (Vanden Abeele et al., 2006). However, Huang et al. reported that Panx1 exhibited no dye transfer or electrical coupling in Panx1-expressing HeLa cells or N2A cells, respectively (Huang et al., 2007), raising concerns that Panx1 was a poor gap junction-channel-forming protein.

In our study, we examined the potential function of Panx1 and Panx3 and found that both pannexins were active in forming single-plasma membrane channels in 293T cells capable of allowing the uptake of sulforhodamine. Importantly, dye uptake in the presence of high calcium concentration would limit the probability of connexin-hemichannel opening in 293T cells, as evidenced by the lack of sulforhodamine uptake in wild-type cells. However, in N2A cells, we did not find any significant evidence of intercellular Panx1 or Panx3 gap junction channels even when the pannexins were highly expressed. Nevertheless, we cannot rule out the possibility that pannexins might require more than the 48 hours used in this study to form functional intercellular channels. This issue remains to be resolved in future studies. Although the role of Panx1 as a single-membrane channel has been established, this is the first evidence that Panx3 might also be effective at assembling into single-membrane channels, albeit when overexpressed. Further insights into the functional role of pannexins might in fact be extracted from studies on their invertebrate orthologs, innexins. In *Drosophila*, the heteromerization of Innexin 2 and Innexin 3 has proven crucial for epithelial organization and polarity of the embryonic epidermis (Lehmann et al., 2006). The knockdown of *innexin 3* causes mislocalization of Innexin 2 and of DE-cadherin, causing cell polarity defects in the epidermis (Lehmann et al., 2006). Therefore, it is possible that two pannexin family members need to be co-expressed to form heteromeric arrangements before they can function as intercellular gap junction channels. In essence, one or more pannexins might play a regulatory role on the function of the other family members in complex protein-interaction networks, similar to what has been reported for some connexin family members (Cottrell et al., 2002).

In summary, our studies suggest that Panx1 and Panx3 fail to meet many of the criteria expected of the connexin family of gap junction proteins. Their diverse subcellular localization pattern, high expression levels in tissues typically deficient in classical gap junctions, glycosylation status and failure to form robust gap junction channels when transiently expressed in N2A cells point to unique cellular functions distinct from connexins. However, essentially all evidence supports their role as single-membrane channels. Nevertheless, the presence of unique molecular species and varied tissue-distribution profiles raises the possibility that they will exhibit a broader range of functions extending beyond their role in forming single-membrane channels; these functions could still include a tissue-specific role in intercellular communication.

## Materials and Methods

### Sequence analysis

The reference sequence (RefSeq) of mouse *Panx1* was validated by the curators at GenBank when we suggested that the current RefSeq (NP_062355, AF207817) did not match the genomic sequence, having several mismatches and one insertion causing a frame shift in the C-terminus. It was then replaced by NP_062355 (NM_019482.2). The RefSeq of *Panx3* was also corrected and replaced by the current NP_766042.2 (NM_172454.2), which shows no mismatches to the mouse genomic sequence. Multiple sequence alignments of the reference sequences of mouse *Panx1* (NM_019482.2) and *Panx3* (NM_172454.2) were done using the ClustalW server from the European Bioinformatics Institute (EBI) (Higgins et al., 1994). Toppred was used for topology and hydrophobicity plot predictions (Claros and Heijne, 1994). Consensus sites for phosphorylation and glycosylation were generated using default settings of NetPhos and NetNGlyc servers (Blom et al., 2004).

### Mouse *Panx1* and *Panx3* expression constructs

Pannexin-specific primers were designed to encompass the entire coding region of the two genes. Panx1 sense (5′-CACCCGGTGCGCCTTGACCAT-3′) and antisense (5′-TAGCACCTGCCAGTCCAGAAT-3′) primers in parallel with Panx3 primers (5′-CATTCTCAGCAGCATCATGTCG-3′ and 5′-TCTTGACTCCCAGACTTCA-CAC-3′) were used to amplify both transcripts with the one-step RT-PCR kit from QIAGEN (Mississauga, ON) from total RNA of mouse osteoblasts, as described previously (McLachlan et al., 2005) and from brain extracted with Trizol (Invitrogen, Burlington, ON). The PCR products were cloned by pGEM-T Easy vector systems (Promega, Madison WI) and full-length products identical to the reported pannexin reference sequences were cloned into expression vectors pEGFP-N1 (Clontech, Palo Alto, CA) or pcDNA3.1+ (Invitrogen, Burlington, ON) and validated by sequencing.

### Generation of pannexin-specific antibodies

Carboxyl-terminal amino acid residues 395-409 (QRVEFKDLDLSSEAA) of mouse Panx1 and amino acid residues 379-392 (KPKHLTQHTYDEHA) of mouse Panx3 were synthesized along with a peptide derived from the tip of the C-terminal sequence of human PANX1 (412-426; NGEKNARQRLLDSSC), tagged with keyhole limpet hemocyanin through an added C-terminal cysteine and used to generate site-directed rabbit polyclonal antibodies by Genemed Synthesis (San Francisco, CA). Sera were collected and tested by immunoblotting and immunolabeling in parallel with pre-immune serum from the same rabbits. Antisera mPanx1B_34 (mouse peptide 395-409) and mPanx3_28 (mouse peptide 379-392) were affinity purified against the specific peptides used in antibody generation by Genemed Synthesis. For the present report, the antibodies derived from mouse pannexin peptides will be noted as ‘anti-Panx1’ and ‘anti-Panx3’, whereas the antibody corresponding to the human PANX1 peptide will be denoted as ‘anti-hPANX1’.

### Cell lines and culture conditions

All media and reagents were obtained from Invitrogen (Burlington, ON), Sigma (St Louis, MO) and BD Biosciences (Mississauga, ON). Normal rat kidney (NRK), rat breast tumor cells (BICR-M1$R_k$), and human embryonic kidney cells (293T) from ATCC (Manassas, VA) were grown in DMEM media supplemented with 10% fetal bovine serum (FBS), 100 units/ml penicillin, 100 μg/ml streptomycin and 2 mM glutamine. Trypsin solution (0.25%, 1 mM EDTA) was purchased from Invitrogen. Mouse neuroblastoma (N2A) cells also from ATCC were grown in Eagle’s minimum media, supplemented with 10% heat-inactivated FBS, 100 units/ml penicillin and 100 μg/ml streptomycin.

### Transfections

For transient transfections, mammalian cells grown to 50-75% confluency in 35- or 60-mm culture dishes were transfected in Opti-MEM1 medium (Invitrogen) containing Lipofectamine2000 and 1 μg of plasmid DNA purified with QIAGEN maxiprep column kit for 4 hours at 37°C. The DNA/Lipofectamine suspension was removed and replaced with culture medium. The efficiency of transfection was determined 48 hours later by visualizing live or fixed cells under a fluorescent microscope. For functional assays of untagged pannexins, each pannexin-encoding construct was co-transfected with a vector encoding red or green fluorescent protein (pDsRed/pEGFP, Invitrogen), as we described (Gong et al., 2006), for selection of live cells projected to also co-express untagged Panx1 or Panx3.

### Immunocytochemistry

Cells grown on coverslips were immunolabeled as previously described (Laird et al., 1995). Briefly, coverslips were fixed with ice-cold 80% methanol and 20% acetone for 20 minutes. Primary antibodies were used in a 1:500 dilution for pannexin antisera and protein disulfide protein (PDI; Stressgen) or 1 μg/ml for affinity-purified anti-pannexin antibodies. For peptide pre-adsorption assays, the diluted antibody was pre-incubated with a 10:1 molar excess of the purified peptide for 30 minutes prior to labeling the cells. Primary antibodies were incubated with the cells for 1 hour at room temperature prior to washing and re-incubation with a donkey anti-rabbit antibody conjugated to Texas Red (Jackson ImmunoResearch, West Grove, PA) or a goat anti-mouse antibody tagged with Texas Red. Coverslips were rinsed in phosphate buffered saline (PBS) and water, counterstained with Hoechst 33342 to denote the nuclei and mounted. Analysis was performed on a Zeiss (Thornwood, NY) LSM 510 inverted confocal microscope.

### Immunoblotting and analysis of post-translational modifications

Cell lysates from control NRK cells or NRK cells expressing untagged or GFP-tagged pannexins were collected from cultures using a Triton-based extraction buffer [1% Triton X-100, 150 mM NaCl, 10 mM Tris, 1 mM EDTA, 1 mM EGTA, 0.5% NP-40, 100 mM NaF, 100 mM sodium orthovanadate, proteinase inhibitor mini-EDTA tablet (Roche-Applied Science, Laval, QC) adjusted to pH 7.4] or a SDS-based extraction buffer (1% SDS in 10 mM Tris HCl, pH 7.4, 100 mM NaF, 100 mM sodium orthovanadate, proteinase inhibitor mini-EDTA tablet). The same protocol, using the Triton-based buffer, was used for extraction of tissue lysates from organs of 3-week-old mice and lymphocyte-rich-thymus tissue from newborn mice. All mice were used in accordance with the Guide for the Care and Use of Laboratory Animals as defined by the University of Western Ontario Animal Care Subcommittee. Each experiment was repeated at least three times, and proteins were quantified using a bicinchonic acid (BCA) assay from Pierce (Rockford, IL). For alkaline phosphatase assays, 10-40 units of shrimp alkaline phosphatase (Fermentas, Burlington, ON) were used to digest cell lysates for 1 hour. Glycosidase assays were performed according to the manufacturer’s instruction, using the N-glycosidase F kit from Roche Applied Science, which included a glycoprotein (transferrin) in parallel as a positive control. Total protein amounts of 20 μg (for cell lysates) or 50 μg (for tissue lysates) were separated on a 10% SDS-PAGE gel and transferred onto nitrocellulose membranes. Membranes were blocked for 30 minutes with Odyssey blocking solution (LiCor, Lincoln, NE) with 0.05% Tween20 in PBS, and incubated overnight at 4°C with either a 1:5000 dilution of anti-pannexins antibodies or 0.2 μg/ml of purified pannexin or Cx43 antibodies. Gel loading controls included probing for the levels of GAPDH or β-actin. For peptide pre-adsorption assays, the diluted antibody was pre-incubated with a 10:1 molar excess of the purified peptide for 30 minutes before performing the western blots. After several washes, the blots were incubated with Alexa-Fluor-680 and -800 secondary antibodies for detection on an Odyssey infrared imaging system (LiCor).

### Brefeldin-A and cycloheximide treatments

BICR-M1$R_k$ cells expressing Cx43-GFP were transfected with cDNAs encoding untagged and GFP-tagged Panx1 and Panx3. The protein secretion blocker brefeldin-A (BFA) (5 μg/ml) was incubated with the cells for 6 hours as described previously (Thomas et al., 2005). Cells were fixed and immunolabeled for pannexins and analyzed under a confocal microscope. In other cases, cells were treated with 20 μg/ml of cycloheximide (CHX; Sigma) to inhibit all protein synthesis, and lysed using the Triton-based buffer at 2, 4, 6 and 8 hours following CHX treatment. Cell lysates were immunoblotted as described above.

### Generation of N-glycosylation mutants for Panx1 and Panx3

Based on the predicted extracellular N-glycosylation consensus sites (Fig. 1B), a site-directed mutagenesis approach was used to generate expression constructs that encoded a change from asparagine (N) to glutamine (Q) at position 254 for Panx1 and position 71 for Panx3. The QuickChange site-directed mutagenesis kit protocol (Stratagene, La Jolla CA) was performed following the manufacturer’s instructions. The resulting clones encoding the Panx1$^{N254Q}$ and Panx3$^{N71Q}$ mutants were verified by sequencing. The constructs encoding the pannexin mutants were transfected into NRK cells for immunolabeling and cell lysates were subjected to immunoblotting and N-glycosidase F treatment as described above.

### Localization of endogenous pannexins

Human facial skin samples were obtained by Bryce Cowan after informed consent from patients attending the Vancouver General Hospital Skin Care Center, University of British Columbia, Vancouver, British Columbia, Canada. During the reconstructive phase, after surgical removal of a cutaneous tumor, samples were taken from discarded normal tissue remote to the primary tumor site. Tissue collection was performed in strict accordance with the ethical principles set for in the Declaration of Helsinki and as instituted at the University of British Columbia. Samples were then fixed in 10% neutral buffered formalin and subsequently embedded in paraffin. Sections (5 μm) were deparaffinized in xylene, rehydrated in graded alcohols, and washed in PBS. For Cx43 and Panx1, antigen retrieval was performed using Vector Antigen Unmasking Solution (Vector Labs, Burlingame, CA) according to the manufacturer’s protocol. Antigen retrieval for Panx3 involved placing slides in 0.01 M sodium citrate buffer pH 6.0 and microwaving for 2.5 minutes at 80% power. Sections were allowed to cool in a closed container for 20 minutes prior to being washed in PBS. Blocking was performed for 1 hour at room temperature in PBS containing 3% bovine serum albumin (BSA) and 0.1% Triton X-100. Primary antibodies were applied to sections for 1.5 hours at 37°C and diluted, where applicable, in PBS with 1% BSA, 0.1% Tween-20 and 0.01% SDS. Primary antibodies included polyclonal antisera recognizing human CX43 (diluted 1:100, Becton Dickenson Biosciences) and human PANX1 (hPANX1) plus the two purified antibodies (2 μg/μl) against mouse Panx1 and Panx3 (diluted 1:100). For peptide competitions, a 10:1 molar ratio of peptide to antibody was used, incubated at room temperature for 30 minutes and applied to sections. Next, the appropriate secondary antibody conjugated to Texas Red (Jackson ImmunoResearch) was applied, diluted 1:100 in PBS with 1% BSA and incubated for 1 hour at room temperature. Hoechst 33342 (1:1000 dilution; Molecular Probes) was used as a nuclear stain. Sections were mounted with Vectashield Mounting Medium (Vector Laboratories). Labeling was visualized with an inverted confocal microscope.

In other studies, spleen tissue from 3-week-old mice was fixed with 10% formalin, dehydrated using a graded ethanol series, rinsed with xylene and embedded in paraffin wax. Tissue sections were cut 5 μm thick, deparaffinized and rehydrated before antigen retrieval with buffer containing sodium citrate at 0.01 mol/L, pH 6.0 in dd$H_20$ and microwaved for a total of 2.5 minutes at 80% power. Tissue samples were blocked with 3% BSA and probed with 10 μg/ml of affinity-purified anti-mPanx1. Texas red-conjugated secondary antibody was used to detect fluorescence and nuclei were stained with Hoechst 33342. Peptide competition was performed using a mixture of 2 μg/ml of peptide and 10 μg/ml of antibody. Slides were mounted and viewed as described above.

Finally, parallel tissues were submerged in hematoxylin for 3 minutes, rinsed with $ddH_20$ and acid alcohol, then submerged in eosin for 45 seconds before rinsing with ethanol and xylene.

### Dye-uptake assays

Stocks of fluorescent dyes were prepared in Dulbecco's-PBS (1×PBS plus 0.1 g/l $CaCl_2$ anhydrous and 0.1 g/l $MgCl_2.6H_2O$, pH 7.4) at 2 mg/ml for sulforhodamine B (558.66 MW, Invitrogen) or 25 mg/ml for the negative control dye dextran-rhodamine (10,000 MW, Invitrogen). Approximately 100,000 untreated 293T cells or cells transfected with constructs encoding pannexins or co-transfected with constructs encoding both pannexins and EGFP were found to exhibit an expression efficiency that exceeded 80%. In some cases, transfection efficiency was further confirmed by immunolabeling for pannexins. At 72 hours post-transfection, confluent cell cultures were rinsed twice with D-PBS on ice and mechanically stimulated with a continuous drip of 800 μl of dye released from a height of 2.5 cm above the culture dish. The stimulation was repeated three times and the dye-covered cells were set on ice for 5 minutes. Ten washes with cold D-PBS were performed with the use of an aspirator and the dishes were examined under a Leica microsystems fluorescent microscope (Richmond Hill, ON) equipped with a Hamamatsu digital camera (Bridgewater, NJ) and OpenLab software (Lexington. MA). Phase-contrast and fluorescent images were collected around the drip target site after light passage through appropriate filter sets using a 20× objective. Five independent transfections were assayed for dye uptake and 293T cells co-transfected with pEGFP were used to confirm the presence of successfully transfected cells in each treatment.

### Dye transfer and patch-clamp electrophysiology

N2A cells were transfected with cDNAs encoding GFP-tagged Cx43, Cx26, Panx1 or Panx3. In other experiments, N2A cells were co-transfected with cDNAs encoding untagged Panx1 or Panx3 and DsRed to denote the Panx-expressing cells. For microinjection of 1% Lucifer yellow dye (dissolved in 0.15 M LiCl), clusters of two or more contacting Panx3-expressing cells were selected as sites of injection. Dye injection was performed until the impinged cell was brightly fluorescent (a few seconds), using a Leica microsystems fluorescent microscope equipped with an Eppendorf microinjection system (McHenry, IL). After 2 minutes, the incidence of transfer was photographed and recorded. As negative controls, wild-type N2A cells were microinjected in parallel.

For dual whole-cell patch-clamp recordings, pannexin- or connexin-expressing N2A cells were prepared and assessed 48 hours post-transfection as previously described (Gong et al., 2006). Isolated N2A cell pairs with distinct GFP-tagged connexins or pannexins, or cell pairs predicted to co-express untagged Panx1 or Panx3 and DsRed were selected for double patch-clamp recordings. Online series resistance compensation at 80% was applied to improve the accuracy in measuring intercellular conductance (Gj), which was determined and presented as mean±s.e.m. Student's *t*-test was performed with Microsoft Excel.

The authors would like to thank Ross Johnson (University of Minnesota) for providing valuable insights into executing the dye uptake studies. This study was supported by the Canadian Institutes of Health Research and Canada Research Chair Program to D.W.L. and D.B.

## References

**Alexander, D. B. and Goldberg, G. S.** (2003). Transfer of biologically important molecules between cells through gap junction channels. *Curr. Med. Chem.* **10**, 2045-2058.

**Bao, L., Locovei, S. and Dahl, G.** (2004). Pannexin membrane channels are mechanosensitive conduits for ATP. *FEBS Lett.* **572**, 65-68.

**Baranova, A., Ivanov, D., Petrash, N., Pestova, A., Skoblov, M., Kelmanson, I., Shagin, D., Nazarenko, S., Geraymovych, E., Litvin, O. et al.** (2004). The mammalian pannexin family is homologous to the invertebrate innexin gap junction proteins. *Genomics* **83**, 706-716.

**Barbe, M. T., Monyer, H. and Bruzzone, R.** (2006). Cell-cell communication beyond connexins: the pannexin channels. *Physiology* **21**, 103-114.

**Beardslee, M. A., Laing, J. G., Beyer, E. C. and Saffitz, J. E.** (1998). Rapid turnover of connexin43 in the adult rat heart. *Circ. Res.* **83**, 629-635.

**Blom, N., Gammeltoft, S. and Brunak, S.** (1999). Sequence- and structure-based prediction of eukaryotic protein phosphorylation sites. *J. Mol. Biol.* **294**, 1351-1362.

**Blom, N., Sicheritz-Ponten, T., Gupta, R., Gammeltoft, S. and Brunak, S.** (2004). Prediction of post-translational glycosylation and phosphorylation of proteins from the amino acid sequence. *Proteomics* **4**, 1633-1649.

**Bruzzone, R., White, T. W. and Paul, D. L.** (1996). Connections with connexins: the molecular basis of direct intercellular signaling. *Eur. J. Biochem.* **238**, 1-27.

**Bruzzone, R., Hormuzdi, S. G., Barbe, M. T., Herb, A. and Monyer, H.** (2003). Pannexins, a family of gap junction proteins expressed in brain. *Proc. Natl. Acad. Sci. USA* **100**, 13644-13649.

**Bruzzone, R., Barbe, M. T., Jakob, N. J. and Monyer, H.** (2005). Pharmacological properties of homomeric and heteromeric pannexin hemichannels expressed in Xenopus oocytes. *J. Neurochem.* **92**, 1033-1043.

**Claros, M. G. and von Heijne, G.** (1994). TopPred II: an improved software for membrane protein structure predictions. *Comput. Appl. Biosci.* **10**, 685-686.

**Cottrell, G. T., Wu, Y. and Burt, J. M.** (2002). Cx40 and Cx43 expression ratio influences heteromeric/ heterotypic gap junction channel properties. *Am. J. Physiol. Cell Physiol.* **282**, C1469-C1482.

**Dvoriantchikova, G. Ivanhov, D., Pestova, A. and Shestopalov, V.** (2006a). Molecular characterization of pannexins in the lens. *Mol. Vis.* **12**, 1417-1426.

**Dvoriantchikova, G., Ivanov, D., Panchin, Y. and Shestopalov, V. I.** (2006b). Expression of pannexin family of proteins in the retina. *FEBS Lett.* **580**, 2178-2182.

**Evans, W. H., De Vuyst, E. and Leybaert, L.** (2006). The gap junction cellular internet: connexin hemichannels enter the signalling limelight. *Biochem. J.* **397**, 1-14.

**Gong, X. Q., Shao, Q., Lounsbury, C. S., Bai, D. and Laird, D. W.** (2006). Functional characterization of a GJA1 frameshift mutation causing oculodentodigital dysplasia and palmoplantar keratoderma. *J. Biol. Chem.* **281**, 31801-31811.

**Goodenough, D. A. and Paul, D. L.** (2003). Beyond the gap: functions of unpaired connexon channels. *Nat. Rev. Mol. Cell Biol.* **4**, 285-294.

**Goodenough, D. A., Goliger, J. A. and Paul, D. L.** (1996). Connexins, connexons, and intercellular communication. *Annu. Rev. Biochem.* **65**, 475-502.

**Higgins, D., Thompson, J., Gibson, T., Thompson, J. D., Higgins, D. G. and Gibson, T. J.** (1994). CLUSTAL W: improving the sensitivity of progressive multiple sequence alignment through sequence weighting, position-specific gap penalties and weight matrix choice. *Nucleic Acids Res.* **22**, 4673-4680.

**Huang, Y., Grinspan, J. B., Abrams, C. K. and Scherer, S. S.** (2007). Pannexin1 is expressed by neurons and glia but does not form functional gap junctions. *Glia* **55**, 46-56.

**John, S. A. and Revel, J. P.** (1991). Connexon integrity is maintained by non-covalent bonds: intramolecular disulfide bonds link the extracellular domains in rat connexin-43. *Biochem. Biophys. Res. Commun.* **178**, 1312-1318.

**Lai, C. P. K., Bechberger, J. F., Thompson, R. J., MacVicar, B. A., Bruzzone, R. and Naus, C. C.** (2007). Tumor-suppressive effects of pannexin 1 in C6 glioma cells. *Cancer Res.* **67**, 1545-1554.

**Laird, D. W.** (1996). The life cycle of a connexin: gap junction formation, removal, and degradation. *J. Bioenerg. Biomembr.* **28**, 311-318.

**Laird, D. W.** (2006). Life cycle of connexins in health and disease. *Biochem. J.* **394**, 527-543.

**Laird, D. W., Puranam, K. L. and Revel, J. P.** (1991). Turnover and phosphorylation dynamics of connexin43 gap junction protein in cultured cardiac myocytes. *Biochem. J.* **273**, 67-72.

**Laird, D. W., Castillo, M. and Kasprzak, L.** (1995). Gap junction turnover, intracellular trafficking, and phosphorylation of connexin43 in brefeldin A-treated rat mammary tumor cells. *J. Cell Biol.* **131**, 1193-1203.

**Lehmann, C., Lechner, H., Loer, B., Knieps, M., Herrmann, S., Famulok, M., Bauer, R. and Hoch, M.** (2006). Heteromerization of innexin gap junction proteins regulates epithelial tissue organization in Drosophila. *Mol. Biol. Cell* **17**, 1676-1685.

**Lippincott-Schwartz, J., Yuan, L. C., Bonifacino, J. S. and Klausner, R. D.** (1989). Rapid redistribution of Golgi proteins into the ER in cells treated with brefeldin A: evidence for membrane cycling from Golgi to ER. *Cell* **56**, 801-813.

**Locovei, S., Bao, L. and Dahl, G.** (2006). Pannexin 1 in erythrocytes: function without a gap. *Proc. Natl. Acad. Sci. USA* **103**, 7655-7859.

**McLachlan, E., Manias, J., Gong, X., Lounsbury, C., Shao, Q., Bernier, S., Bai, D. and Laird, D.** (2005). Functional characterization of oculodentodigital dysplasia-associated Cx43 mutants. *Cell Commun. Adhes.* **12**, 279-292.

**Panchin, Y., Kelmanson, I., Matz, M., Lukyanov, K., Usman, N. and Lukyanov, S.** (2000). A ubiquitous family of putative gap junction molecules. *Curr. Biol.* **10**, R473-R474.

**Pelegrin, P. and Surprenant, A.** (2006). Pannexin-1 mediates large pore formation and interleukin-1beta release by the ATP-gated P2X7 receptor. *EMBO J.* **25**, 5071-5082.

**Phelan, P.** (2005). Innexins: members of an evolutionarily conserved family of gap-junction proteins. *Biochim. Biophys. Acta* **1711**, 225-245.

**Saez, J. C., Retamal, M. A., Basilio, D., Bukauskas, F. F. and Bennett, M. V.** (2005). Connexin-based gap junction hemichannels: gating mechanisms. *Biochim. Biophys. Acta* **1711**, 215-224.

**Solan, J. L. and Lampe, P. D.** (2005). Connexin phosphorylation as a regulatory event linked to gap junction channel assembly. *Biochim. Biophys. Acta* **1711**, 154-163.

**Thomas, T., Jordan, K., Simek, J., Shao, Q., Jedeszko, C., Walton, P. and Laird, D. W.** (2005). Mechanisms of Cx43 and Cx26 transport to the plasma membrane and gap junction regeneration. *J. Cell Sci.* **118**, 4451-4462.

**Thompson, R. J., Zhou, N. and MacVicar, B. A.** (2006). Ischemia opens neuronal gap junction hemichannels. *Science* **312**, 924-927.

**Vanden Abeele, F., Bidaux, G., Gordienko, D., Beck, B., Panchin, Y. V., Baranova, A. V., Ivanov, D. V., Skryma, R. and Prevarskaya, N.** (2006). Functional implications of calcium permeability of the channel formed by pannexin 1. *J. Cell Biol.* **174**, 535-546.

**Willecke, K., Eiberger, J., Degen, J., Eckardt, D., Romualdi, A., Guldenagel, M., Deutsch, U. and Sohl, G.** (2002). Structural and functional diversity of connexin genes in the mouse and human genome. *Biol. Chem.* **383**, 725-737.